

## Supporting Information

# Microheterogeneity in Aqueous Acetonitrile Solution Probed by Soft X-ray Absorption Spectroscopy

Masanari Nagasaka,<sup>\*,†,‡</sup> Hayato Yuzawa,<sup>†</sup> and Nobuhiro Kosugi<sup>†,‡</sup>

<sup>†</sup>Institute for Molecular Science, Myodaiji, Okazaki 444-8585, Japan

<sup>‡</sup>SOKENDAI (The Graduate University for Advanced Studies), Myodaiji, Okazaki 444-8585, Japan

\*E-mail: nagasaka@ims.ac.jp

<b>Table of Contents</b>	<b>Page</b>
<b>Theoretical Method</b>	S2
<b>Results and Discussion</b>	
S1. O K-edge XAS of Water Gas and Condensed Acetonitrile Solution	S3
S2. Inner-Shell Calculations of Water Enclosed in Acetonitrile	S3
S3. C and N K-edge XAS of Acetonitrile in Gas and Liquid Phases	S4
S4. Radial Distribution Function of Liquid Acetonitrile	S4
S5. Inner-Shell Calculations of Acetonitrile in Gas and Liquid Phases	S5
S6. Radial Distribution Function of Acetonitrile with Water	S6
<b>References</b>	S9

## Theoretical Method

### *Molecular Dynamics Simulation*

Molecular dynamics (MD) simulations were performed by using the program package GROMACS 5.1.2.<sup>1</sup> The potential of acetonitrile molecule is described by the OPLS-AA force field,<sup>2-3</sup> and that of water molecule is TIP5P.<sup>4</sup> The temperature is controlled by the Nosé-Hoover thermostat method.<sup>5-6</sup> The pressure is adjusted by the Parrinello-Rahman method.<sup>7</sup> The simulations were performed at a time step of 1 fs with a periodic boundary condition and the partial-mesh Ewald method.<sup>8</sup> Randomly distributed structures were optimized by the simulations, which run during 100 ps at 100 K in the canonical ( $NVT$ ) ensemble, 100 ps at 200 K and 1 atm in the isobaric-isothermal ( $NpT$ ) ensemble, and 2 ns at 25 °C and 1 atm in the  $NpT$  condition. In the dilute acetonitrile solution ( $x = 0.001$ ), the system contains 10 acetonitrile and 9990 water molecules in a cubic box. The equilibrium structures were obtained by sampling the structures every picosecond at 25 °C and 1 atm during a simulation time of 10 ns. For the equilibrium structures of liquid acetonitrile, 500 acetonitrile molecules were sampled every picosecond at 25 °C and 1 atm during a simulation time of 2 ns.

## Results and Discussion

### S1. O K-edge XAS of Water Gas and Condensed Acetonitrile Solution

Figure S1 shows O K-edge XAS spectra of water gas and condensed acetonitrile solution at  $x = 0.9$  in  $(\text{CH}_3\text{CN})_x(\text{H}_2\text{O})_{1-x}$ . The  $4a_1$  peak in water gas corresponds to the pre-edge peak of liquid water, and the  $2b_2$  peak is the main-edge peak, respectively. These peaks show sharp profiles since water molecules in the gas phase have no interactions with other molecules. On the other hand, the main-edge peak in the condensed acetonitrile solution shows a sharp profile, which has been also observed in the previous studies.<sup>9-11</sup> The pre-edge and main-edge peaks in the condensed acetonitrile solution at  $x = 0.9$  show higher energy shifts by 526 meV and by 392 meV compared to those of water gas, respectively.

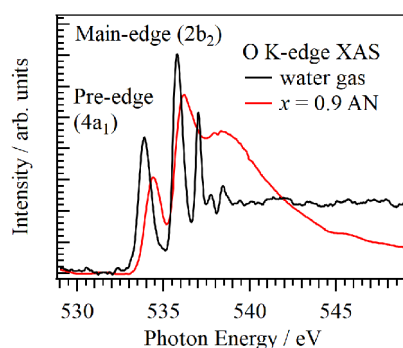


**Figure S1.** O K-edge XAS spectra of water gas and condensed acetonitrile solution at  $x = 0.9$ .

### S2. Inner-Shell Calculations of Water Enclosed in Acetonitrile

Figure S2 shows calculated O K-edge inner-shell spectra of water gas, water enclosed in two acetonitrile (2 DP), and liquid water. Molecular distances and alignments between water and acetonitrile were determined from radial distribution function (RDF) shown in Section S6. In the 2 DP model, the  $4a_1$  and  $2b_2$  peaks show higher energy shifts by 303 meV and by 317 meV, respectively, compared to those of water gas. These energy shifts are consistent with the experimental results shown in Figure S1. It means that the sharp profile of the main-edge peak is derived from water molecules surrounded by acetonitrile molecules. The  $4a_1$  peak in the 2 DP model is lowered by  $-346$  meV than that of liquid water. It is consistent with the decrease of the pre-edge peak energy ( $-206$  meV) from  $x = 0.0$  to  $x = 0.9$  at the O K-edge XAS of aqueous acetonitrile solutions  $(\text{CH}_3\text{CN})_x(\text{H}_2\text{O})_{1-x}$  shown in Figure 1. Although the calculated energy shift is slightly smaller than the experimental value, it would be explained that water molecules are not completely isolated in acetonitrile molecules at  $x = 0.9$ .

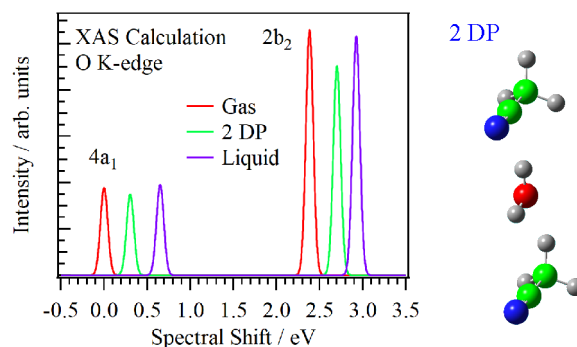


**Figure S2.** Calculated O K-edge spectral shifts of the 4a<sub>1</sub> and 2b<sub>2</sub> peaks for water enclosed in two acetonitrile (2 DP) and liquid water relative to the 4a<sub>1</sub> peak of water gas. The inset shows the 2 DP model structure, where core excited water molecule forms the DP structure with two acetonitrile molecules.

### S3. C and N K-edge XAS of Acetonitrile in Gas and Liquid Phases

Figure S3 shows C and N K-edge XAS of acetonitrile in gas and liquid phases. As observed in the previous studies,<sup>12-13</sup> the transition peaks from 1s electrons to C≡N π\* orbitals were obtained by XAS in both C and N K-edges. The C≡N π\* peaks at the C K-edge show higher energy shifts by 119 meV from gas to liquid phases. On the other hand, the energy shift of the C≡N π\* peaks at the N K-edge is small (16 meV) compared to that at the C K-edge.

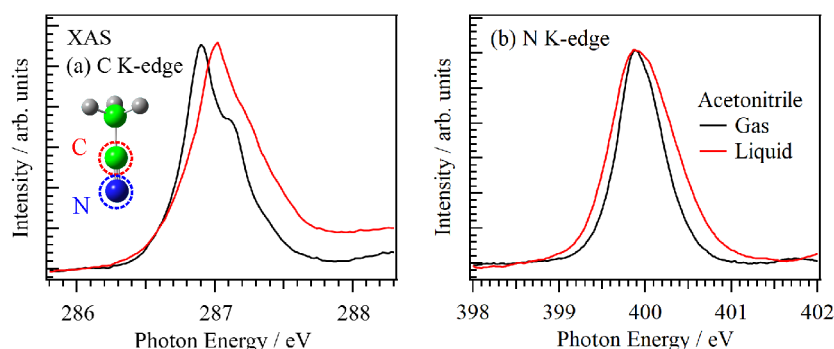


**Figure S3.** XAS spectra of acetonitrile in gas and liquid phases at (a) C and (b) N K-edges. The inset shows the core excited C and N atoms in the acetonitrile molecule.

### S4. Radial Distribution Function of Liquid Acetonitrile

Figure S4(a) shows two-dimensional (2D) RDF between C atoms of C≡N group in acetonitrile molecules (C-C) obtained by the MD simulations of liquid acetonitrile ( $x = 1.0$ ). The vertical axis is the angle  $\theta$  between C atoms of C≡N group in acetonitrile molecules. The maximum intensity of the 2D RDF shows that the angle  $\theta$  is around 80°. Then, we have calculated 2D RDF C-C at  $70^\circ < \theta < 90^\circ$ , as shown in Figure

S4(b). The vertical axis is the angle  $\varphi$  between C $\equiv$ N group in acetonitrile molecule ( $f_1$ ) and that in another molecule ( $f_2$ ). The intensity of the 2D RDF shows a maximum when the angle  $\varphi$  is around 180°. These results clearly suggest that acetonitrile molecules show the antiparallel structures in neat acetonitrile, as shown in the inset of Figure S4.

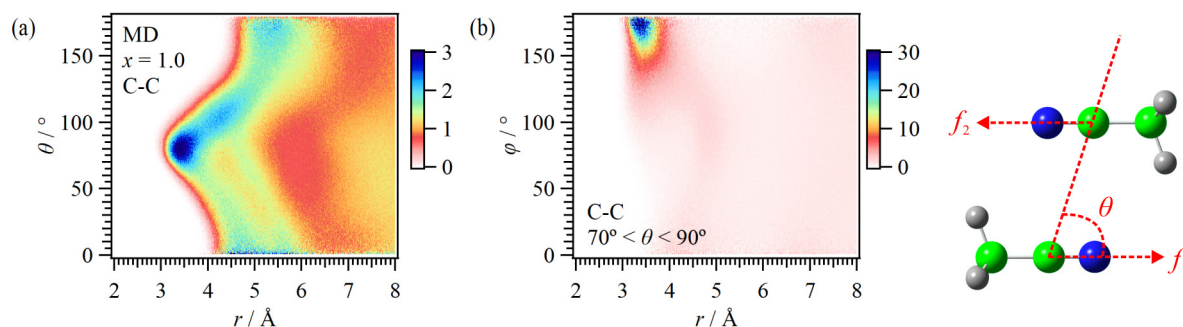


**Figure S4.** (a) 2D RDF between C atoms of C $\equiv$ N group in acetonitrile molecules (C-C). The inset shows the definition of the angle  $\theta$  between acetonitrile molecules. (b) 2D RDF C-C at  $70^\circ < \theta < 90^\circ$ , where  $\varphi$  is the angle between C $\equiv$ N group in acetonitrile molecule ( $f_1$ ) and that in another molecule ( $f_2$ ).

## S5. Inner-Shell Calculations of Acetonitrile in Gas and Liquid Phases

Liquid acetonitrile forms one- and two-dimensional chain structures with the antiparallel displaced C $\equiv$ N groups in acetonitrile, whose coordination number is 2.<sup>14-15</sup> For understanding the dipole interaction between acetonitrile chains in liquid phase, we have performed the inner-shell calculations at the C and N K-edges with different coordination numbers of acetonitrile, as shown in Figure S5.

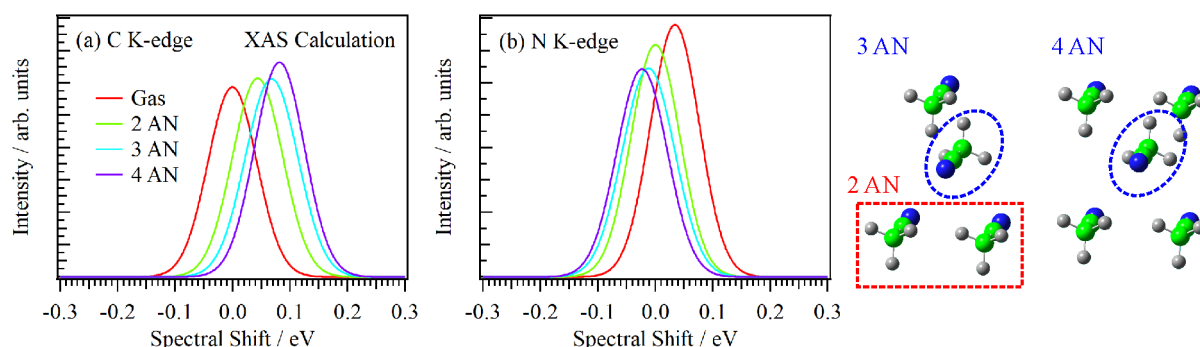


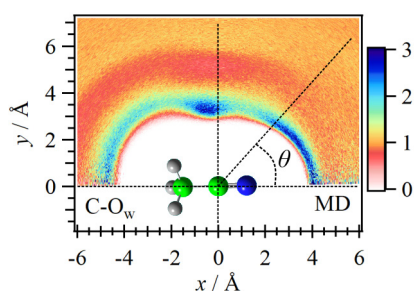
**Figure S5.** Calculated spectral shifts of several models for liquid acetonitrile at (a) C and (b) N K-edges relative to the gas peaks. The inset shows model structures used for the inner-shell calculations, where the core excited acetonitrile molecules, which are marked in blue circles, are surrounded by 2, 3, and 4 acetonitrile molecules in the 2 AN, 3 AN, and 4 AN model, respectively.

The 2 AN model represents the acetonitrile chain structure, where acetonitrile is surrounded by two acetonitrile molecules. The C K-edge inner-shell spectrum of the 2 AN model shows a higher energy shift by 43 meV from gas, whereas N K-edge spectrum shows a lower energy shift by  $-34$  meV. The higher energy shift in C K-edge is caused by the exchange interaction of the  $C\equiv N \pi^*$  electron with surrounding molecules, and the lower energy shift in N K-edge is caused by the electrostatic stabilization arising from the polarization induced by the ionized core.<sup>16</sup> These trends are partially consistent with the XAS experiments of gas and liquid phases shown in Figure S3. However, the calculated C K-edge energy shift of the 2 AN model (43 meV) is smaller than that obtained by the experiment (119 meV).

Then, we consider the dipole interactions between the acetonitrile chains, where the core excited acetonitrile molecules are surrounded by 3 and 4 acetonitrile molecules in the 3 AN and 4 AN model, respectively. In the calculated C K-edge spectra, the energy shifts become larger by increasing the coordination numbers, which are 68 meV at the 3 AN model and 81 meV at the 4 AN model. In the calculated N K-edge spectra, on the other hand, the energy shifts at the 3 AN and 4 AN model are  $-46$  meV and  $-57$  meV, respectively. By increasing the coordination numbers, the inner-shell spectra at the N K-edge show lower energy shifts, but these energy shifts are smaller than those at the C K-edge. These results suggest that the coordination numbers should be above 2 to reproduce the energy shift of the  $C\equiv N \pi^*$  peaks from gas to liquid phases. It means that acetonitrile chains would be gathered by the dipole interactions in the liquid phase.

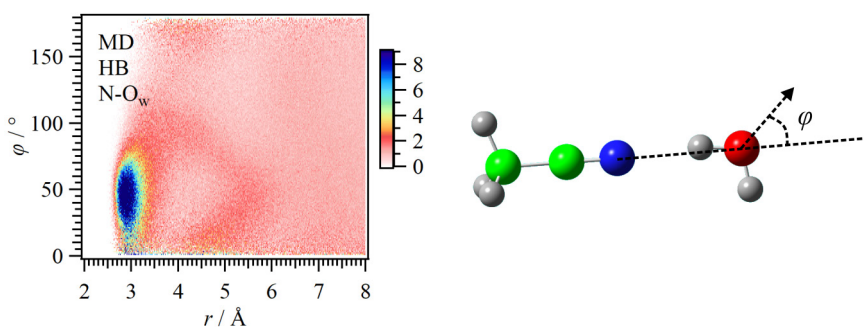
## S6. Radial Distribution Function of Acetonitrile with Water

Figure S6 shows 2D RDF between C atoms of  $C\equiv N$  groups in acetonitrile and O atoms in water ( $C-O_w$ ) obtained by the MD simulations of dilute acetonitrile solutions at  $x = 0.001$ . The maximum intensities of water are found at the parallel direction ( $\theta = 0^\circ$ ) and  $\theta = 100^\circ$  relative to the direction of the  $C\equiv N$  group in acetonitrile.



**Figure S6.** 2D RDF between C atoms of  $C\equiv N$  groups in acetonitrile and O atoms in water ( $C-O_w$ ). The inset shows the definition of the angle  $\theta$  between acetonitrile and water.

For the hydrogen bond (HB) structure, we have collected water molecules within the angle  $0^\circ < \theta < 50^\circ$  relative to the direction of the  $C\equiv N$  group in acetonitrile. Figure S7 shows 2D RDF between N atoms of  $C\equiv N$  group in acetonitrile and O atoms in water ( $N-O_w$ ) at  $0^\circ < \theta < 50^\circ$ . The vertical axis is the angle  $\varphi$  between  $N-O_w$  and symmetry axis of water as shown in the inset. The maximum intensity of the 2D RDF indicates that the distance  $N-O_w$  is 2.91 Å and the angle  $\varphi$  is  $46^\circ$ . It means that water molecules form the HB structures with N atoms of  $C\equiv N$  group in acetonitrile.



**Figure S7.** 2D RDF between N atoms of  $C\equiv N$  group in acetonitrile and O atoms in water ( $N-O_w$ ) in the HB structure. The inset shows the definition of the angle  $\varphi$ , which is the angle between  $N-O_w$  and symmetry axis of water.

For the dipole (DP) structure, we have collected water molecules within the angle  $80^\circ < \theta < 120^\circ$  relative to the direction of the  $C\equiv N$  group in acetonitrile. Figure S8 shows the 2D RDF between C atoms of  $C\equiv N$  group in acetonitrile and O atoms in water ( $C-O_w$ ) at  $80^\circ < \theta < 120^\circ$ . The vertical axis is the angle  $\varphi$  between  $C-O_w$  and symmetry axis of water as shown in the inset. The maximum intensity of the 2D RDF shows that the distance  $C-O_w$  is 3.48 Å and the angle  $\varphi$  is  $120^\circ$ . We found that the acceptor sites in water molecules point the  $C\equiv N$  group in acetonitrile with the DP interactions.

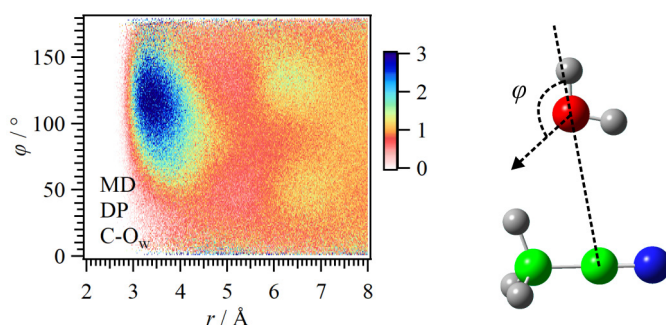


**Figure S8.** 2D RDF between C atoms of  $C\equiv N$  group in acetonitrile and O atoms in water ( $C-O_w$ ) in the DP structure. The inset shows the definition of the angle  $\varphi$ , which is the angle between  $C-O_w$  and symmetry axis of water.

Figure S9 shows  $N(\theta)/\sin\theta$  as a function of  $\theta$ , in which the coordination numbers  $N(\theta)$  at different angles  $\theta$  are obtained from the minimal points of the first coordination peaks ( $r = 5.44 \text{ \AA}$ ) in RDF. If the coordination number shows no angular dependence,  $N(\theta)/\sin\theta$  becomes unity. Since  $N(\theta)/\sin\theta$  around  $\theta = 100^\circ$  is larger than that around  $\theta = 0^\circ$ , the population of the DP structure is higher than that of the HB structure.

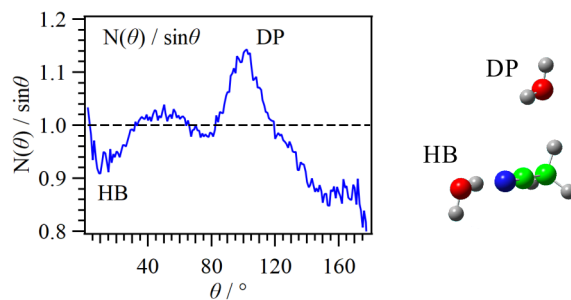


**Figure S9.**  $N(\theta)/\sin\theta$  as a function of  $\theta$ . The HB structure is below unity, whereas the DP structure is above unity. The inset shows schematics of the HB and DP structures.

## References

- (1) Abraham, M. J.; Murtola, T.; Schulz, R.; Páll, S.; Smith, J. C.; Hess, B.; Lindahl, E. GROMACS: High Performance Molecular Simulations through Multi-Level Parallelism from Laptops to Supercomputers. *SoftwareX* **2015**, *1-2*, 19-25.
- (2) Jorgensen, W. L.; Tirado-Rives, J. Potential Energy Functions for Atomic-Level Simulations of Water and Organic and Biomolecular Systems. *Proc. Natl. Acad. Sci. U. S. A.* **2005**, *102*, 6665-6670.
- (3) Caleman, C.; van Maaren, P. J.; Hong, M. Y.; Hub, J. S.; Costa, L. T.; van der Spoel, D. Force Field Benchmark of Organic Liquids: Density, Enthalpy of Vaporization, Heat Capacities, Surface Tension, Isothermal Compressibility, Volumetric Expansion Coefficient, and Dielectric Constant. *J. Chem. Theory Comput.* **2012**, *8*, 61-74.
- (4) Mahoney, M. W.; Jorgensen, W. L. A Five-Site Model for Liquid Water and the Reproduction of the Density Anomaly by Rigid, Nonpolarizable Potential Functions. *J. Chem. Phys.* **2000**, *112*, 8910-8922.
- (5) Nosé, S. A Unified Formulation of the Constant Temperature Molecular Dynamics Methods. *J. Chem. Phys.* **1984**, *81*, 511-519.
- (6) Hoover, W. G. Canonical Dynamics: Equilibrium Phase-Space Distributions. *Phys. Rev. A* **1985**, *31*, 1695-1697.
- (7) Parrinello, M.; Rahman, A. Polymorphic Transitions in Single Crystals: A New Molecular Dynamics Method. *J. Appl. Phys.* **1981**, *52*, 7182-7190.
- (8) Darden, T.; York, D.; Pedersen, L. Particle Mesh Ewald: An  $N \cdot \log(N)$  Method for Ewald Sums in Large Systems. *J. Chem. Phys.* **1993**, *98*, 10089-10092.
- (9) Huang, N.; Nordlund, D.; Huang, C.; Bergmann, U.; Weiss, T. M.; Pettersson, L. G. M.; Nilsson, A. X-ray Raman Scattering Provides Evidence for Interfacial Acetonitrile-Water Dipole Interactions in Aqueous Solutions. *J. Chem. Phys.* **2011**, *135*, 164509.
- (10) Lange, K. M.; Könnicke, R.; Soldatov, M.; Golnak, R.; Rubensson, J.-E.; Soldatov, A.; Aziz, E. F. On the Origin of the Hydrogen-Bond-Network Nature of Water: X-ray Absorption and Emission Spectra of Water-Acetonitrile Mixtures. *Angew. Chem. Int. Ed.* **2011**, *50*, 10621-10625.
- (11) Tokushima, T.; Horikawa, Y.; Takahashi, O.; Arai, H.; Sadakane, K.; Harada, Y.; Takata, Y.; Shin, S. Solvation Dependence of Valence Electronic States of Water Diluted in Organic Solvents Probed by Soft X-ray Spectroscopy. *Phys. Chem. Chem. Phys.* **2014**, *16*, 10753-10761.
- (12) Hitchcock, A. P.; Tronc, M.; Modelli, A. Electron Transmission and Inner-Shell Electron Energy Loss Spectroscopy of CH<sub>3</sub>CN, CH<sub>3</sub>NC, CH<sub>3</sub>SCN, and CH<sub>3</sub>NCS. *J. Phys. Chem.* **1989**, *93*, 3068-3077.
- (13) Carniato, S.; Taïeb, R.; Kukk, E.; Luo, Y.; Brena, B. N-K near-Edge X-Ray-Absorption Fine Structures of Acetonitrile in Gas Phase. *J. Chem. Phys.* **2005**, *123*, 214301.
- (14) Radnai, T.; Itoh, S.; Ohtaki, H. Liquid Structure of N,N-Dimethylformamide, Acetonitrile, and Their 1 : 1 Molar Mixture. *Bull. Chem. Soc. Jpn.* **1988**, *61*, 3845-3852.
- (15) Takamuku, T.; Tabata, M.; Yamaguchi, A.; Nishimoto, J.; Kumamoto, M.; Wakita, H.; Yamaguchi, T. Liquid Structure of Acetonitrile-Water Mixtures by X-ray Diffraction and Infrared Spectroscopy. *J. Phys. Chem.*

*B* **1998**, *102*, 8880-8888.

(16) Nagasaka, M.; Hatsui, T.; Setoyama, H.; Rühl, E.; Kosugi, N. Inner-Shell Spectroscopy and Exchange Interaction of Rydberg Electrons Bound by Singly and Doubly Charged Kr and Xe Atoms in Small Clusters. *J. Electron Spectrosc. Relat. Phenom.* **2011**, *183*, 29-35.